Supporting Information

Supported Gold Nanoparticles for Alcohols Oxidation in Continuous-Flow Heterogeneous Systems

Barbara Ballarin,[a] Davide Barreca,[b] Elisa Boanini,[c] Maria Cristina Cassani,[a] Paolo Dambruoso,[d] Alessandro Massi,[e] Adriana Mignani,[a] Daniele Nanni,[a*] Chiara Parise,[a] and Anna Zaghi[e]*

[a]Dipartimento di Chimica Industriale "Toso Montanari", Università di Bologna, Via Risorgimento 4, I-40136, Bologna, Italy; [b]CNR-ICMATE and INSTM, Department of Chemistry, Padova University, Via F. Marzolo, 1, I-35131, Padova, Italy; [c]Dipartimento di Chimica "Giacomo Ciamician", Università di Bologna, Via Selmi 2, I-40126, Bologna, Italy; [d]Istituto per la Sintesi Organica e la Fotoreattività, Consiglio Nazionale delle Ricerche, Via P. Gobetti, 101, I-40129, Bologna, Italy; [e]Dipartimento di Scienze Chimiche e Farmaceutiche, Università di Ferrara, Via Fossato di Mortara 17, I-44121, Ferrara, Italy.

Including pages S1-S13

Figures S1-S8

References 1-10

List of Abbreviations

Au_{NPs}: gold nanoparticles

SiO_2@Yne: silica functionalized with alkynyl-carbamate moieties

Au/SiO_2@Yne: gold nanoparticles supported on functionalized silica

Al_2O_3@Yne: aluminum oxide functionalized with alkynyl-carbamate moieties

Au/Al_2O_3@Yne: gold nanoparticles supported on functionalized aluminum oxide

TiO_2@Yne: titanium oxide functionalized with alkynyl-carbamate moieties

Au/TiO_2@Yne: gold nanoparticles supported on functionalized titanium oxide

OS@Yne: inorganic oxides functionalized with alkynyl-carbamate moieties

Au/OS@Yne: gold nanoparticles supported on functionalized oxide supports

TGA: Thermogravimetric Analysis; wt %: weight percentage

TEM: Transmission Electron Microscopy

ATR-FTIR: Total Reflectance Fourier Transformed Infrared Spectroscopy

XPS: X-ray Photoelectron Spectroscopy

GC: Gas Chromatography

1. Characterization of Au/OS@Yne

The amount of gold present on the different samples was determined with flame atomic absorption spectroscopy (AAS, Thermo Scientific) in air-acetylene flame with a wavelength of 242.8 nm and a spectral band-width of 0.5 nm. The analyses were conducted on the solid samples by comparison with the calibration line obtained with six calibration standards, prepared by dilution to 50 mL of different amounts of a concentrated $HAuCl_4 \cdot 3H_2O$ aqueous solution. The samples of **Au/SiO_2@Yne** were prepared by first dissolving the solid (ca. 8 mg) in 1 mL of NaOH 2 M and 2 mL of aqua regia in an ultrasonic bath at 60 °C, then further 4.5 mL of NaOH were added to achieve the total dissolution of silica. Finally, the solution was diluted with water to a volume of 50 mL. The samples of **Au/Al_2O_3@Yne** and **Au/TiO_2@Yne** were prepared by dissolving the solid (ca. 10 mg) in 10 mL of HNO_3 65%, 0.5 mL of H_2SO_4 68%, and 1 mL of H_2O_2 30% and keeping the mixture in a microwave oven (Start Synth Microwawe Synthesis Labstation) at 200 °C for 1 h. Then, the obtained solution was diluted with water to a final volume of 25 mL. The solids used for AAS measurements and catalytic tests were weighted with a Mettler Toledo AT 21 Comparator balance.

TGA analysis

Thermogravimetric analyses were carried out using a Perkin Elmer TGA-7. Heating was performed in a platinum crucible at a rate of 10 °C/min from 40 °C to 900 °C. The samples weights were in the range 5–10 mg. In the thermograms reported in Figure S1 the red line represents the weight loss percentage while the dotted line is the derivative of weight loss percentage.

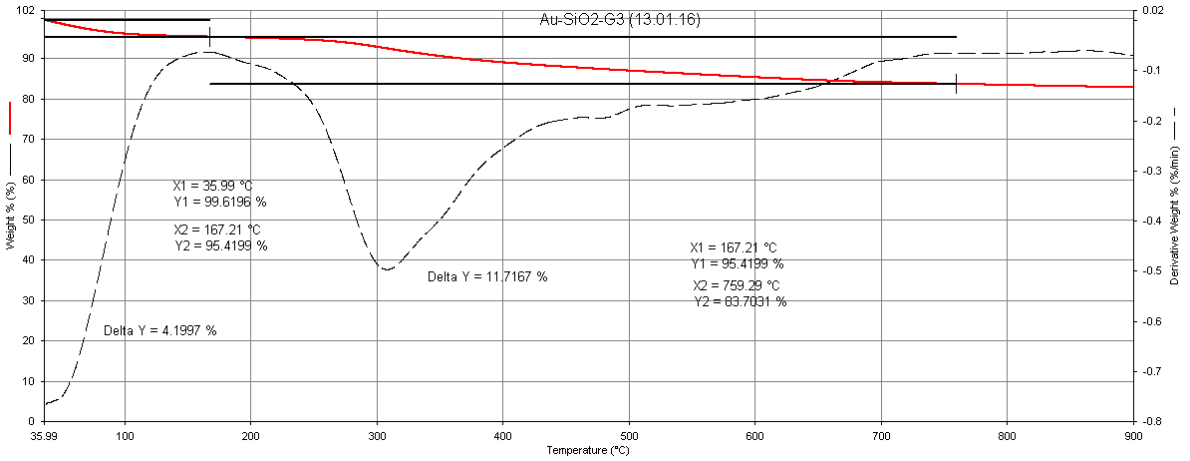

(a)

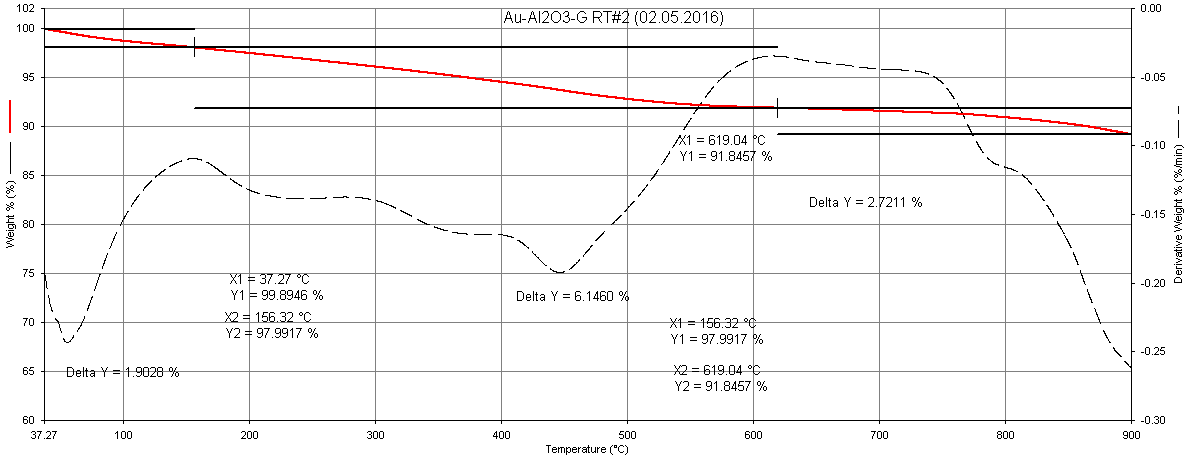

(b)

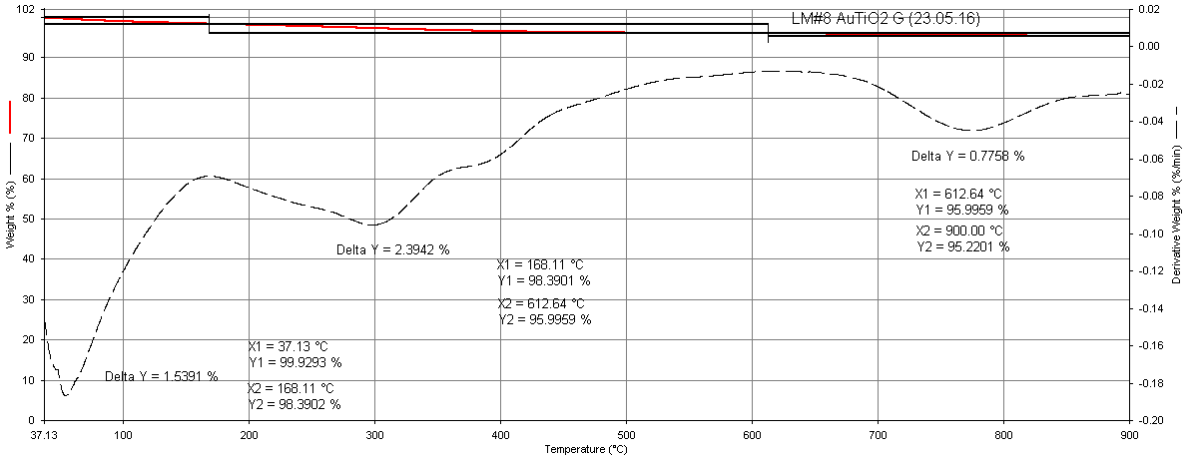

(c)

Figure S1. TGA analyses of (a) **Au/SiO_2@Yne**; (b) **Au/Al_2O_3@Yne**; (c) **Au/TiO_2@Yne**.

TEM analysis

For TEM investigations a Philips CM 100 transmission electron microscope operating at 80 kV was used. To prepare the sample a drop of the suspension was transferred onto holey carbon foils supported on conventional copper micro-grids. The ImageJ® picture analyzer software[1] was used to

estimate the average Au_{NPs} dimensions, averaging the measurements over at least 100 data points per sample.

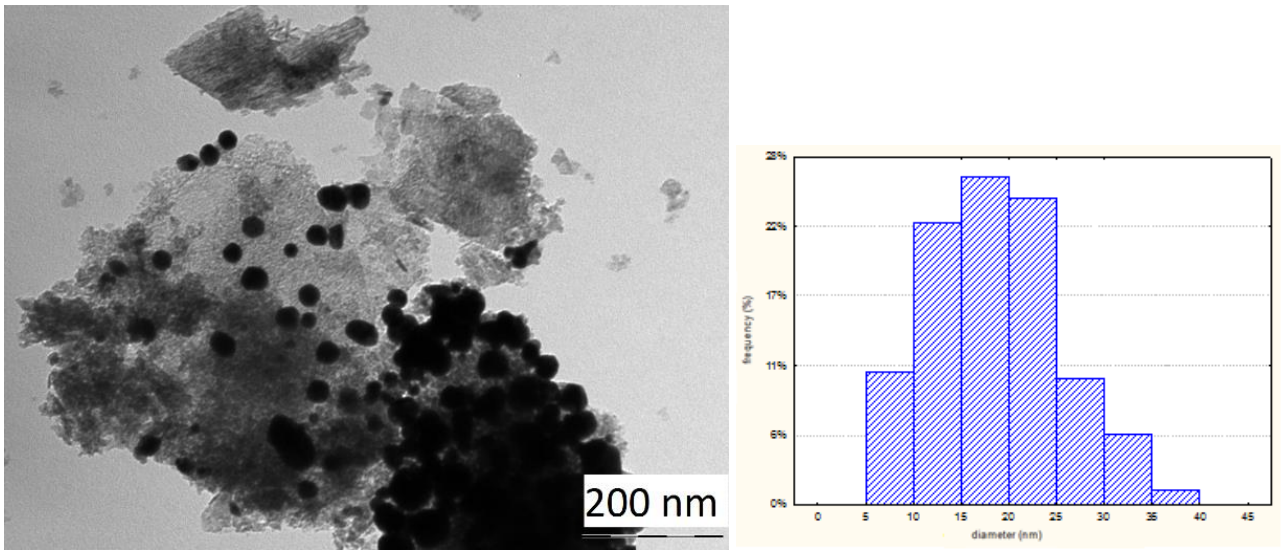

(a)

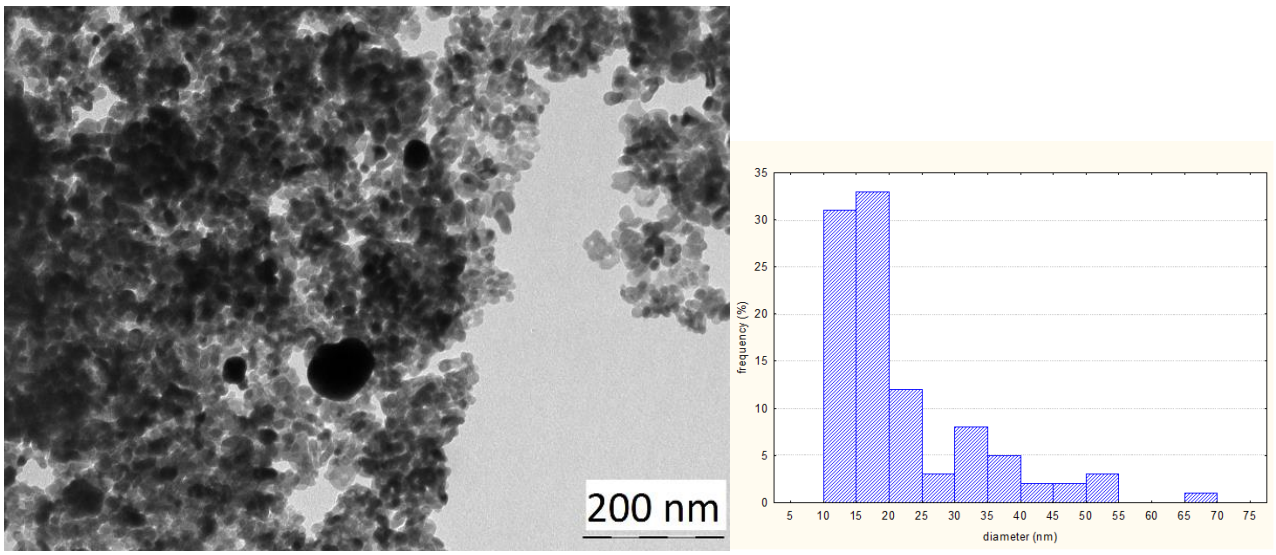

(b)

Figure S2. TEM images and particles size distribution of (a) **Au/Al_2O_3@Yne** (18 ± 7 nm); (b) **Au/TiO_2@Yne** (large distribution).

XPS analysis

The surface O1s photopeaks for the target specimens are displayed in Figure S3a. For **Au/SiO_2@Yne**, a single band centered at BE = 532.5 eV confirmed the presence of a silica-like network, as also supported by the Si2p position (BE = 103.3 eV; Figure S3b)[2,3] despite overlapped contributions from chemisorbed –OH moieties could not be excluded.[4] For **Au/Al_2O_3@Yne**, two different signals contributed to the O1s peak, and were attributed to lattice O in Al_2O_3 (**VI**; BE = 531.1 eV, 58% of the total oxygen signal) and to adsorbed oxygen/chemisorbed -OH groups (**VII**; BE = 532.4 eV) due to atmospheric exposure. The Al2p photoelectron peak position (74.5 eV, Figure S3c) also agreed to a good extent with previous values reported for alumina.[5] Finally, in the case of **Au/TiO_2@Yne**, the O1s surface peak could be decomposed by means of two different bands, located at BE = 530.0 eV (80% of the total oxygen) and 531.7 eV. While the former was ascribed to lattice oxygen in TiO_2 (in line with the energy location of the main spin orbit component of the Ti2p signal, BE($Ti2p_{3/2}$) = 458.8 eV, Figure S3d), the second oxygen band could be attributed both to adsorbed surface -OH groups and adsorbed oxygen;[2,6,7] Estimation of the O/M ratios (with M = Si, Al, Ti for **Au/SiO_2@Yne**, **Au/Al_2O_3@Yne** and **Au/TiO_2@Yne**) yielded values of 2.7, 2.3 and 2.8, respectively, higher than the stoichiometric ones expected for the bare supports due to both air exposure and surface functionalization.

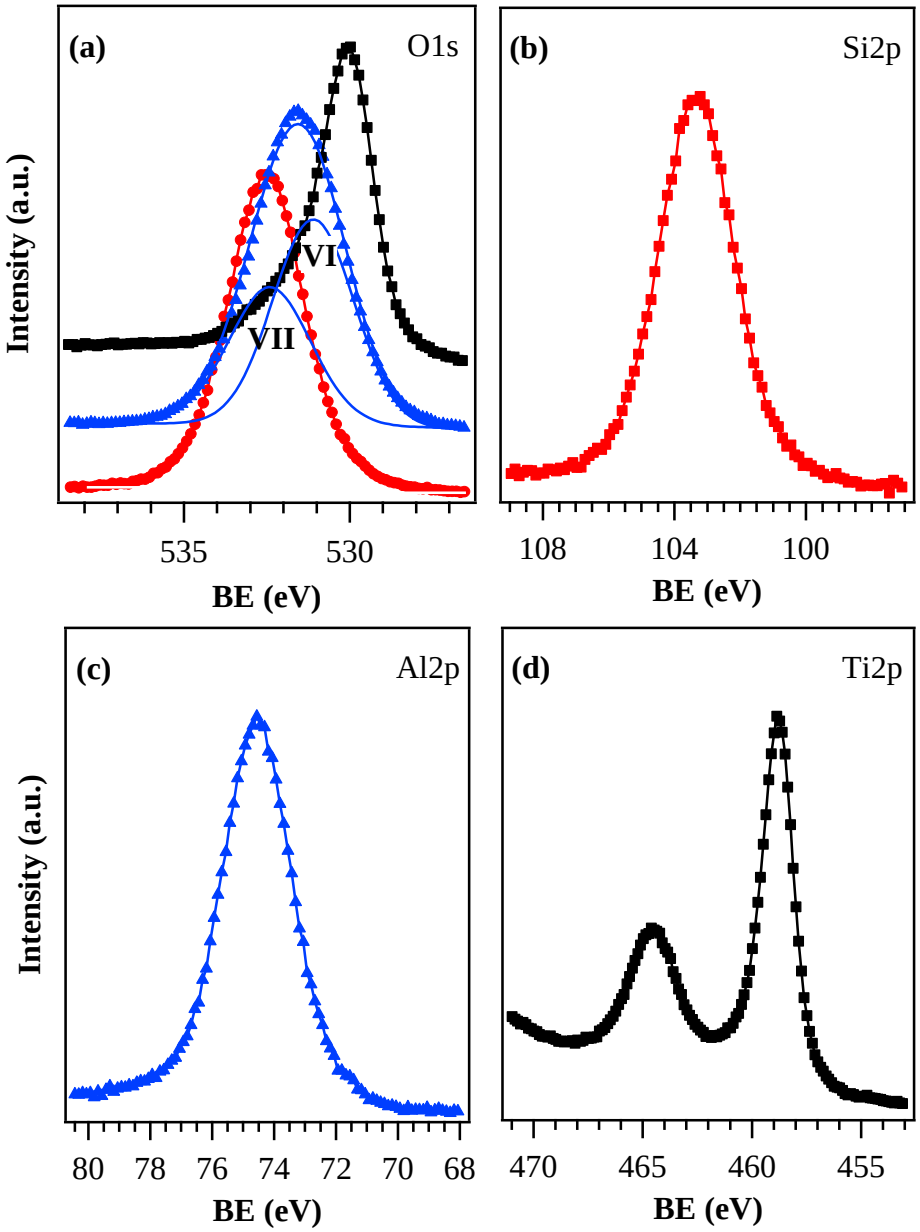

Figure S3. Surface XPS signals for O1s **(a)**, Si2p **(b)**, Al2p **(c)** and Ti2p **(d)**. Color codes: red, sample **Au/SiO_2@Yne**; blue, sample **Au/Al_2O_3@Yne**; black, sample **Au/TiO_2@Yne.**

.

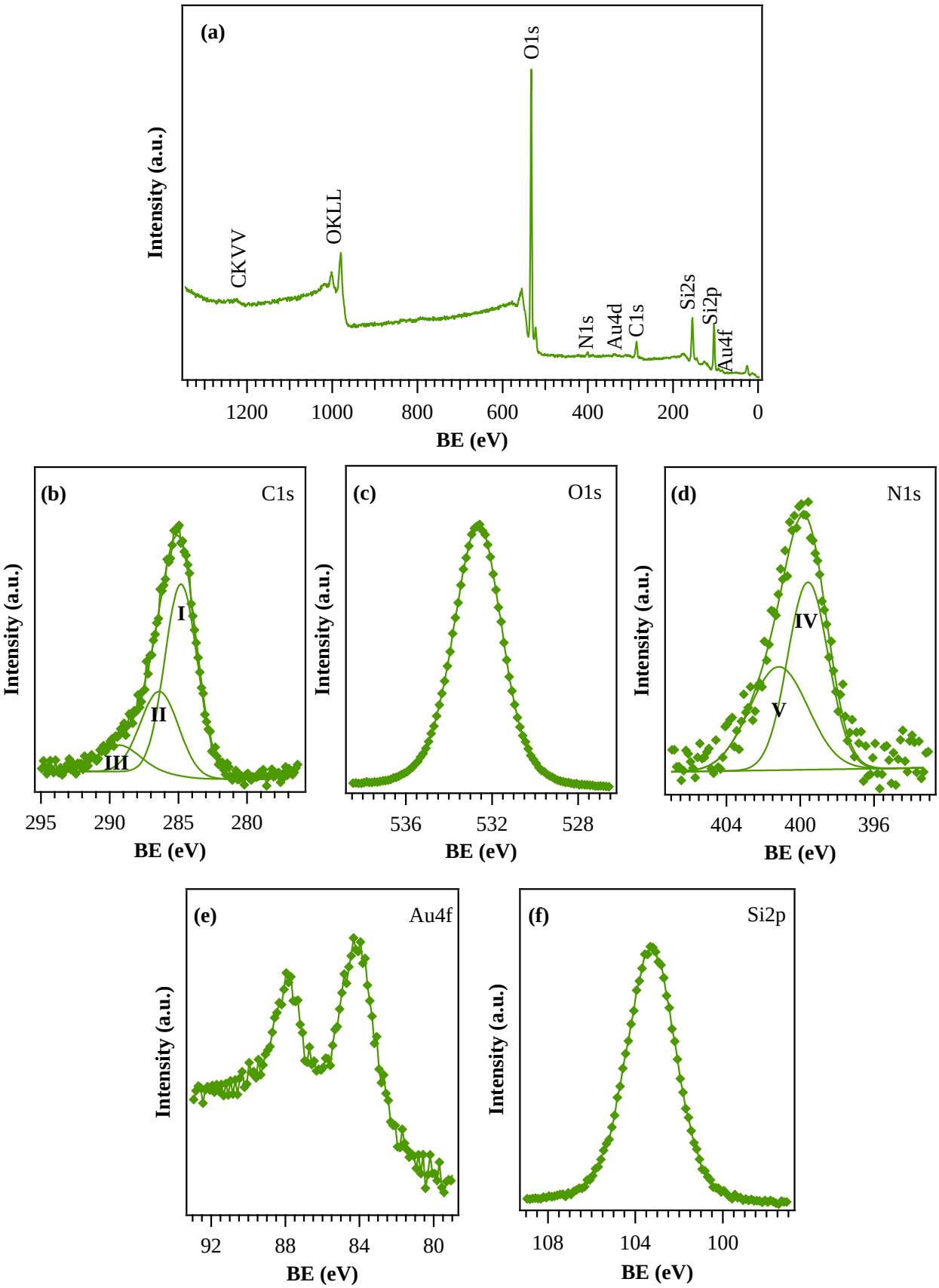

Figure S4. Surface wide-scan XP spectra **(a)** and representative C1s **(b)**, O1s **(c)**, N1s **(d)**, Au4f **(e)** and Si2p **(f)** signals for **Au/SiO$_2$@Yne** after catalytic tests.

ATR-FTIR analysis

ATR-FTIR analysis was performed with a Perkin Elmer Spectrum Two spectrophotometer, equipped with an Universal ATR accessory, in the range 4000-400 cm^{-1} with a resolution of 0.5 cm^{-1}. Pristine and modified oxides powders were directly analyzed after being ground in a mortar performing 20 scans for each analysis.

The ATR-FTIR spectra of **SiO_2@Yne** and **Au/SiO_2@Yne** (the latter showed in Figure S5 as a representative example) were recorded and showed no substantial differences: in the region between 1250 and 400 cm^{-1} the fingerprint of SiO_2[8] was found (with the main band at 1064 cm^{-1} ascribable to the stretching of Si-O-Si), whereas the presence of the carbamate moiety was evidenced by the appearance of two bands at 1703 and 1531 cm^{-1} respectively associated to the C=O stretching and the N-H bending of PPTEOS. The spectrum of **Au/Al_2O_3@Yne** presented a large band between 1000 and 400 cm^{-1} related to Al-O-Al stretchings[9] and the two bands attributed to the organic functionalization at 1698 and 1539 cm^{-1}; analogously the spectrum of **Au/TiO_2@Yne** showed an intense band related to the Ti-O vibrations[10] at 400-600 cm^{-1}, along with the two bands located at 1697 cm^{-1} and 1534 cm^{-1}.

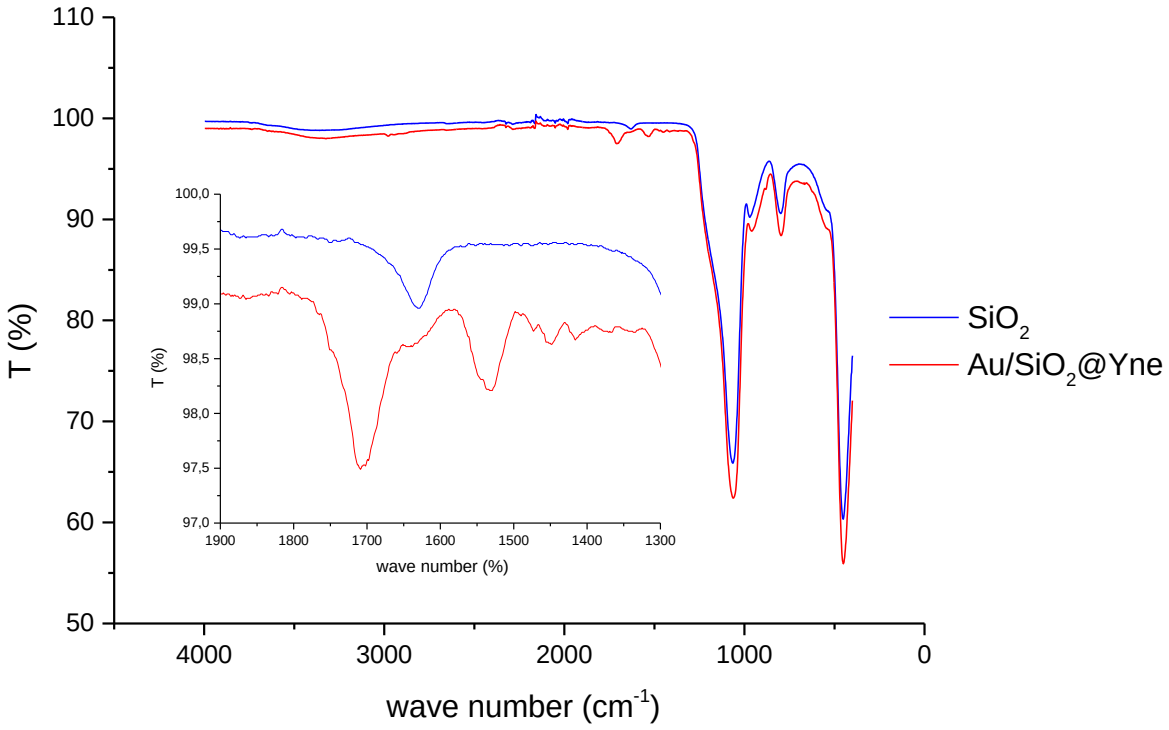

Figure S5. ATR-FTIR spectra of bare SiO_2 and **Au/SiO$_2$@Yne**.

2. Alcohol oxidation catalyzed by Au/OS@Yne

^{1}H-NMR analysis

The catalytic activity of **Au/OS@Yne** was evaluated in the oxidation of various alcohols, determining the final conversion by ^{1}H-NMR analysis. NMR spectra were recorded in $CDCl_3$ using a Varian Gemini XL 300 (^{1}H 300.1 MHz, ^{13}C 75.5 MHz) instrument; chemical shifts were referenced internally to residual solvent peaks. An absolute error of ±5% affects NMR integrations. As a representative example, Figure S6 displays the NMR spectrum recorded at the end of the oxidation of 1-phenylethanol with **Au/SiO$_2$@Yne**.

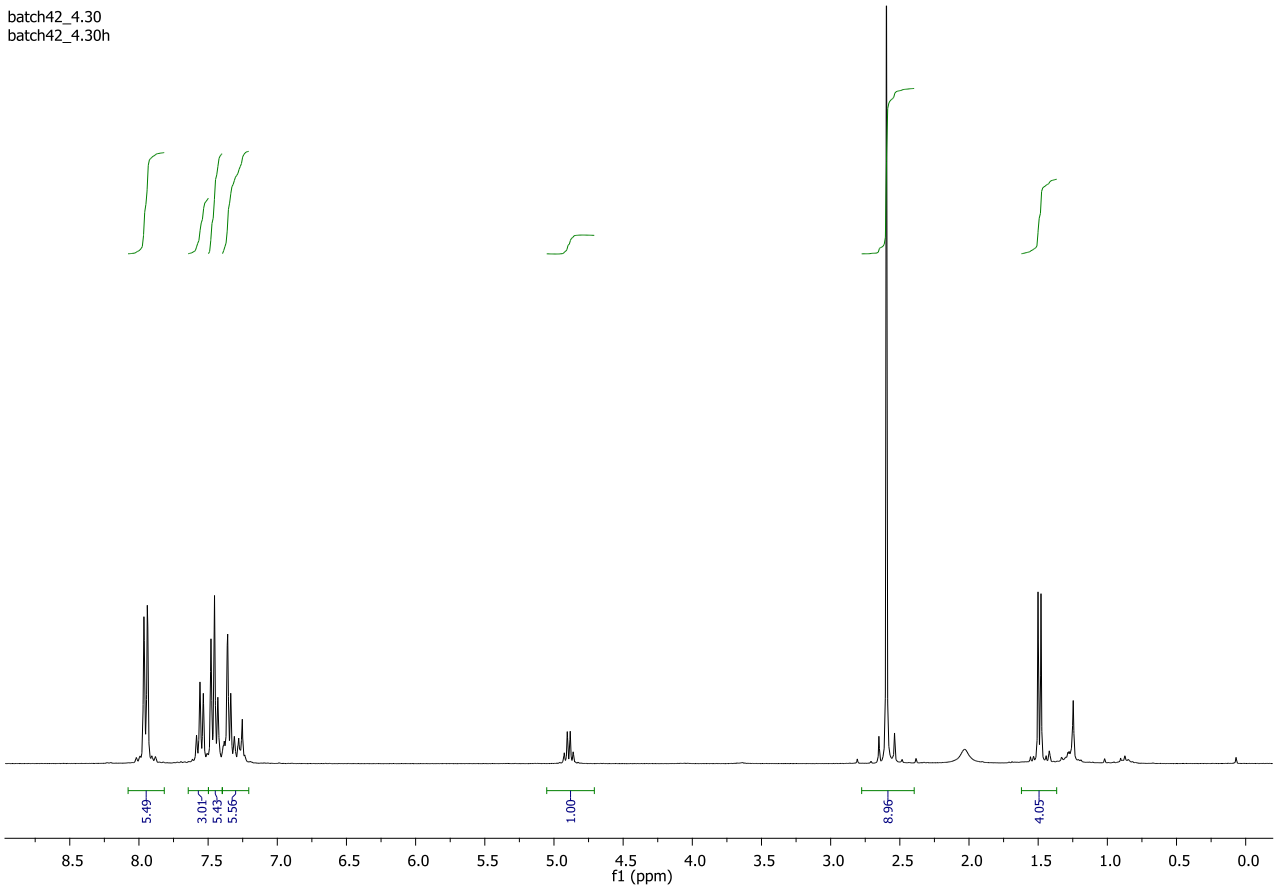

Figure S6. ^{1}H-NMR spectrum of the oxidation reaction of 1-phenylethanol to acetophenone.

GC analysis

In the case of benzyl alcohol the final conversion and selectivity were also determined by GC analysis, using an Agilent Technologies 7890A GC system. Calibration lines for benzyl alcohol, benzoic acid and benzaldehyde were obtained after injection of four aqueous solutions at a known concentration, employing 1,7-heptanediol as internal standard. The samples were introduced into the column using a split mode (30:1). The oven temperature during the analysis was: initial temperature of 50 °C held for 1 minute, a first ramp at 20 °C min^{-1} to 150 °C and finally a ramp at 35 °C min^{-1} up to 250 °C.

Continuous-flow set-up scheme

The continuous-flow experiments were carried out in the system represented in Figure S7.

Figure S7. Scheme of the continuous-flow set-up.

Recycling tests

After being reused in three cycles of oxidation, the catalyst **Au/SiO$_2$@Yne** was analyzed by TEM microscopy as shown in Figure S8.

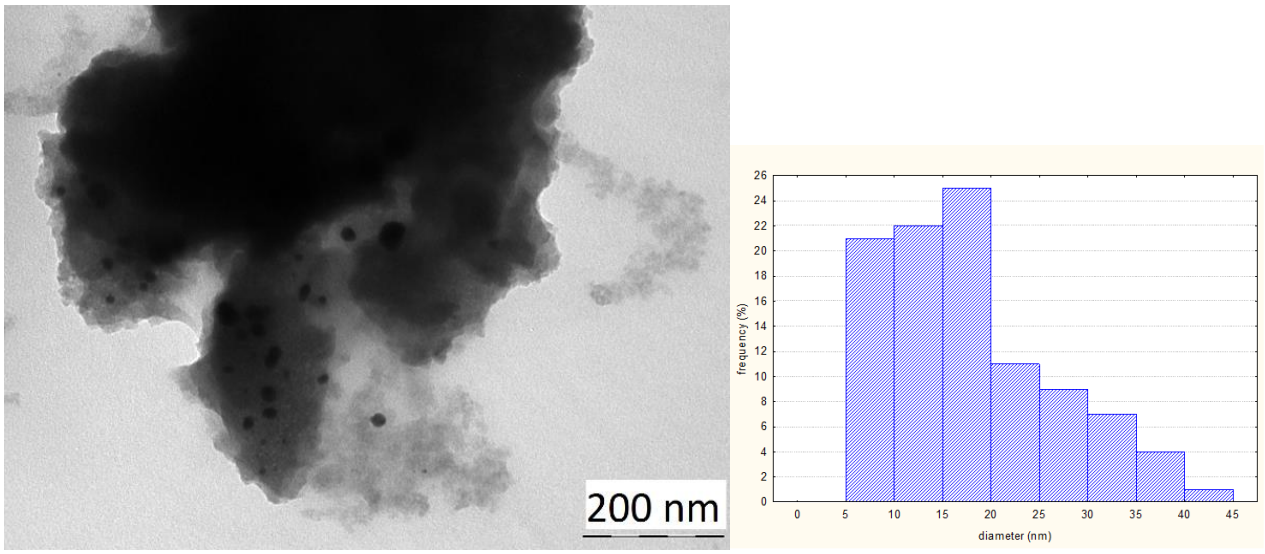

Figure S8. TEM images and particles size distribution of reused **Au/SiO$_2$@Yne**.

(1) http://imagej.nih.gov/ij/ accessed May 2015.

(2) Briggs, D.; Seah, M. P.; *Practical Surface Analysis by Auger and X-ray Photoelectron Spectroscopy*; Wiley: New York, 2nd edn. 1990.

(3) Barreca, D.; Gasparotto, A.; Maccato, C.; Maragno, C.; Tondello, E.; Rossetto, G. Low-temperature PECVD of transparent $SiO_xC_yH_z$ thin films. *Chem. Vapor. Depos.* **2007**, *13*, 205-210.

(4) Barreca, D.; Gasparotto, A.; Maccato, C.; Tondello, E.; Rossetto, G. A soft plasma enhanced-chemical vapor deposition process for the tailored synthesis of SiO_2 films. *Thin Solid Films* **2008**, *516*, 7393-7399.

(5) Zhao, C.; Li, B.; Du, J.; Chen, J.; Li, Y. Microstructure and optical absorption property of Au nanoparticles and Au, Ag bimetal nanoparticles separately dispersed Al_2O_3 composite films. *J. Alloy Compd.* **2017**, *691*, 772-777.

(6) http://srdata.nist.gov/xps

(7) Fittipaldi, M.; Gombac, V.; Gasparotto, A.; Deiana, C.; Adami, G.; Barreca, D.; Montini, T.; Martra, G.; Gatteschi, D.; Fornasiero, P.. Synergistic role of B and F dopants in promoting the photocatalytic activity of rutile TiO_2. *ChemPhysChem* **2011**, *12*, 2221-2224.

(8) Ding, Y.; Chu, X.; Hong, X.; Zou, P.; Liu, Y. The infrared fingerprint signals of silica nanoparticles and its application in immunoassay. *Appl. Phys. Lett.*, **2012**, *100*, 0137011 - 0137013.

(9) Jiao, X.; Li, H.; Li, L.; Xiao, F.; Zhao, N., Wei, W. Synthesis and CO_2 capture properties of mesoporous MgAl(O) sorbent. *RSC Adv*. **2014**, *4*, 47012-47020. Suelson, A. Bending frequency of gaseous aluminum oxide. *J. Phys. Chem.* **1970**, *74*, 2574–2575.

(10) Primet, M.; Pichat, P.; Mathieu, M. V. Infrared study of the surface of titanium dioxides. II. Acidic and basic properties. *J. Phys. Chem*. **1971**, *75*, 1221-1226.